

# Squeezing a Helium Nanodroplet with a Rydberg Electron<sup>†</sup>

F. Ancilotto,<sup>\*,‡</sup> M. Pi,<sup>§</sup> R. Mayol,<sup>§</sup> M. Barranco,<sup>§</sup> and K. K. Lehmann<sup>||</sup>

INFN-CNR DEMOCRITOS National Simulation Center and Dipartimento di Fisica “G. Galilei”,  
Università di Padova, via Marzolo 8, I-35131 Padova, Italy, Departament ECM, Facultat de Física, and  
IN<sup>2</sup>UB, Universitat de Barcelona. Diagonal 647, 08028 Barcelona, Spain, and  
Department of Chemistry and Physics, University of Virginia, 22904-4319 Charlottesville, Virginia

Received: July 31, 2007; In Final Form: October 10, 2007

We have investigated, by means of density functional theory, the structure of a “scolium”, that is, an electron circulating around a positively charged <sup>4</sup>He nanodroplet, temporarily prevented from neutralization by the helium–electron repulsion. The positive ion core resides in the center of the nanodroplet where, as a consequence of electrostriction, a strong increase in the helium density with respect to its bulk value occurs. The electron enveloping the <sup>4</sup>He cluster exerts an additional electrostatic pressure which further increases the local <sup>4</sup>He density around the ion core. We argue that under such pressure, sufficiently small <sup>4</sup>He nanodroplets may turn solid. The stability of a scolium with respect to electron–ion recombination is investigated.

## 1. Introduction

It has been proposed in the past the possibility of creating long-lived surface Rydberg atoms<sup>1,2</sup> consisting of a positive ion adsorbed below the liquid helium surface, while the external Rydberg electron is located outside the helium and cannot penetrate inside the liquid because of the positive energy barrier for electron penetration,  $V_0 \sim 1$  eV. A similar system, that is, a metastable Rydberg atom where the positive ion is located under a solid hydrogen surface, has been also proposed.<sup>3</sup> Similarly, a system made by an electron circulating around a positively charged <sup>4</sup>He nanodroplet, prevented from neutralization by the helium–electron repulsion, was studied by Golov and Sekatskii,<sup>4</sup> and named Scolium after Giacinto Scoles.<sup>5,6</sup>

Recent experiments<sup>7</sup> on the Rydberg nature of high-lying electronically excited states of small <sup>4</sup>He clusters seem to point to the presence of Rydberg states of the same nature as those originally proposed by Golov,<sup>4</sup> that is, an excited electron largely localized outside the He cluster, under the attraction of a positive He ion in the interior of it.

The temporary trapping of photoelectrons into Rydberg states largely located outside the <sup>4</sup>He cluster has also been invoked in the interpretation of photoelectron imaging of helium nanodroplets.<sup>8</sup> Other works on highly electronically excited states of helium clusters and nanodroplets have recently been reported.<sup>9,10</sup>

Different routes than that used in ref 7 could be followed for a practical realization of a scolium. One possibility consists of a two-step process where first a <sup>4</sup>He cluster doped with a positive ion is created, and later, an electron is picked up. The first step has been proved possible in recent experiments where metal ions have been attached to helium droplets by means of laser evaporation techniques,<sup>11</sup> allowing isolation of charged particles inside <sup>4</sup>He clusters at temperatures below 1 K. The electron attachment to <sup>4</sup>He droplets can be realized similarly as in the

experiments reported in refs 12–14 where a low-energy electron beam is crossed with a helium cluster beam.

A second way for producing a scolium could be through a gentle collision between an atom, previously excited into a high- $n$  Rydberg state and a pure <sup>4</sup>He nanodroplet.

Yet, another way of realizing in practice a scolium could follow the excitation in a Rydberg state of an neutral atom impurity deeply bound to the surface of a <sup>4</sup>He nanodroplet like, for instance, an alkaline-earth atom.<sup>15</sup> Following the excitation process, the electron wavefunction could be forced outside the interface region, while the ion core will sink toward the interior of the <sup>4</sup>He nanodroplet because of electrostriction, leading eventually to a state where the electron wavefunction completely surrounds the nanodroplet, remaining largely confined outside its surface.

The excitation into Rydberg states of silver atoms initially embedded in the center of <sup>4</sup>He nanodroplets has been experimentally studied, but the impurity atom was found to move, after the excitation, to the surface of the droplet and eventually desorb.<sup>16</sup> An experiment is planned to look for these Rydberg atoms using Pb<sup>+</sup> cations.<sup>17</sup>

Interestingly, the results of a more recent experiment, where the excited-state dynamics of silver atoms in <sup>4</sup>He nanodroplets have been investigated,<sup>18</sup> can be interpreted as providing some evidence for the existence of a scolium.<sup>19</sup>

The positive ion core in a scolium resides in the bulk of the nanodroplet where, as a consequence of electrostriction, it strongly perturbs the <sup>4</sup>He density around it. In particular, a local increase in the helium density with respect to its bulk value appears near the ion site, whose magnitude depends on the strength of the ion–He interaction potential.<sup>20–22</sup>

Strongly attractive ions tend to form a solid-like structure, the so-called “snowball”, characterized by a very inhomogeneous, solid-like helium density distribution in the surroundings of the ion. Alkali ions are believed to belong to this category.<sup>21,22</sup> In contrast, singly charged alkaline-earth cations, due to their larger radii and lower strength interaction with the He atoms, are expected to produce a cavity surrounded by compressed, less structured, and likely not solidified helium.<sup>23,24</sup>

<sup>†</sup> Part of the “Giacinto Scoles Festschrift”.

<sup>\*</sup> Corresponding author.

<sup>‡</sup> Università di Padova.

<sup>§</sup> Universitat de Barcelona.

<sup>||</sup> University of Virginia.

The recent discovery that positive ions can be captured in helium nanodroplets<sup>11</sup> promises an extension to charged particles of experimental techniques which proved extraordinarily fruitful for neutral species in He nanodroplets.<sup>6,25</sup> Ionization of <sup>4</sup>He clusters by electron impact has also been achieved, producing clusters with a He<sup>+</sup> ion in their center.<sup>26</sup>

The local order around different positive ions has been theoretically studied both in liquid <sup>4</sup>He<sup>23,27</sup> and <sup>4</sup>He clusters,<sup>23</sup> with the aim of computing the local structure and the hydrodynamical contribution to the effective masses of positive ions moving in liquid <sup>4</sup>He (see also ref 28). More recently, a path integral-ground state Monte Carlo method<sup>29</sup> has been used to study the structure of positive alkali and alkaline-earth ions in small <sup>4</sup>He clusters.<sup>24</sup>

In a scolium, the outer electron enveloping the nanodroplet exerts an additional electrostatic pressure on it, which further increases the local <sup>4</sup>He density around the ion core. One may thus speculate that, under the combined effect of electrostriction and of the electrostatic pressure exerted by the Rydberg electron, the helium local density could exceed the freezing density, causing the whole droplet, or a substantial part of it, to become solid. The occurrence of a structural liquid–solid transition around positive ions immersed in bulk liquid helium as a consequence of an increase of the applied pressure has been proposed long ago.<sup>20</sup> Here, we suggest the possibility of a similar effect in an ion-doped <sup>4</sup>He nanodroplet due to the electrostatic pressure exerted by the outer electron. To support this speculation, we present density functional (DF) calculations addressing the structure of a scolium and provide some evidence that, under the mentioned combined effect, sufficiently small <sup>4</sup>He nanodroplets might indeed become solid.

We note that we will be using in the paper the term “Rydberg” in a somewhat nonstandard way. Conventional Rydberg electron states are excited states with high values of the principal quantum number and consequently large values of the orbit radius. Here, we rather consider the lowest energy state of an electron confined outside the <sup>4</sup>He cluster, since this is the electronic state that compresses the droplet the most.

The paper is organized as follows. In section 2, we present a simple model of a scolium, showing that an increase of pressure inside the nanodroplet is expected because of the electrostatic compression exerted by the outer electron which might exceed the <sup>4</sup>He freezing pressure for sufficiently small clusters. Section 3 illustrates the results of more detailed DF calculations, where the structure of a scolium made of a <sup>4</sup>He nanodroplet doped with a Be<sup>+</sup> ion is studied. In section 4, we address the issue of the stability of a scolium with respect to ion–electron recombination. Section 5 contains a brief summary.

## 2. Simple Model for a Scolium

We discuss in this section the results of simple model calculations, aimed at showing that the electrostatic pressure exerted by an electron in a scolium can indeed produce in the interior of the nanodroplet density values exceeding the freezing density for bulk <sup>4</sup>He. We use here essentially the same model used to compute the energy levels of the Rydberg electron in a simple model of a scolium.<sup>4</sup> For the sake of clarity, we summarize in the following the main ingredients of such a model. It is assumed that the electron resides outside a homogeneous spherical <sup>4</sup>He droplet of radius  $R$  characterized by a sharp surface, which contains a positive unit charge located in the center. Electrostriction effects are neglected; that is, the positive charge does not influence the structure of the droplet.

The He–ion interaction will be properly included in the more realistic calculations presented in the next section.

The electron potential energy is assumed to be  $V(r) = V_0 - e^2/(\epsilon r)$  inside the cluster, where  $\epsilon = 1.057$  is the liquid <sup>4</sup>He dielectric constant and  $V_0$  is the height of the barrier preventing the electron from entering the helium droplet. This barrier is experimentally known to be  $V_0 \sim 1$  eV for the penetration of a quasi-free electron into liquid <sup>4</sup>He at saturation conditions.<sup>30</sup> Outside the cluster, the electron potential energy is simply  $V(r) = -e^2/r$ . We neglect the contribution due to the attractive image forces arising from the polarization of the He atoms caused by the electron, which are very small compared with the electron–ion interaction.

We have numerically solved the radial Schrödinger equation for an electron subjected to the potential described above (see eq 6 of ref 4) and computed the energy  $E_e$  of the lowest ( $n = 1$ ,  $l = 0$ ) electron state for a droplet of radius  $R$  made of  $N$  helium atoms. The total energy of a scolium (cluster + ion + electron) is approximately given, as a function of  $R$ , by

$$E(R) = E_e + E_{\text{He}} + 4\pi R^2 \sigma \quad (1)$$

The <sup>4</sup>He energy  $E_{\text{He}} = \Omega f_b(\rho)$  in the second term ( $\Omega$  being the volume of the system) is obtained from the bulk <sup>4</sup>He energy density<sup>31</sup> at the given  $\rho = 3N/(4\pi R^3)$ , where  $f_b$  includes a two-body He–He interaction of Lennard-Jones type, conveniently screened at short distances, and correlation terms due to the short-range part of the He–He interaction. The third term in eq 1 is the cost for the formation of the cluster surface,  $\sigma$  being the liquid <sup>4</sup>He surface tension.

The outside electron compresses the droplet and reduces the diffuseness of its surface. Hence, the surface tension is higher than that of a pure droplet. On the basis of the actual compression of the interface region, which is an output of the more detailed DF calculations presented in the next section, we estimated the increase in  $\sigma$  from the calculated interface width and from the results of ref 32. Our estimate is  $\sigma \sim 0.4 \text{ K } \text{\AA}^{-2}$ . For a given <sup>4</sup>He density  $\rho$ , we actually use a simple rescaled potential barrier  $V_0(\rho/\rho_0)$  when computing  $E_e$  in eq 1 to account for the increased density of the compressed cluster. This linear rescaling<sup>33</sup> is an acceptable approximation, within the simple model discussed in this section.

The results of our model calculations indicate that, for a given  $N$ , there is a minimum in the total energy, as computed above, as a function of the droplet radius  $R$ . This follows from a simple physical interpretation of eq 1, that is, that the electron–ion attractive potential favors a smaller, denser cluster, in competition with the He–He repulsive short-range interaction.

From the equilibrium radius corresponding to the minimum energy, we can compute the equilibrium density and thus the pressure from the bulk equation of state  $P = -f_b(\rho) + \rho \partial f_b(\rho)/\partial \rho$  for a given number of <sup>4</sup>He atoms in the droplet. We show in Figure 1 the calculated density and pressure as a function of  $N$ . It appears that the pressure in the interior of small <sup>4</sup>He clusters exceeds the freezing pressure ( $P \sim 25$  bar) for bulk <sup>4</sup>He.

The model discussed in this section is based on a very simple description of the <sup>4</sup>He density. In real systems, however, the actual <sup>4</sup>He cluster density is far more complex, being characterized by a diffuse surface (whose profile affects the behavior of the enveloping electron) and by a highly inhomogeneous <sup>4</sup>He density around the ion caused by electrostriction. In particular, the additional effect of electrostriction might favor the formation of solid-like structures in clusters of larger sizes than those predicted by the simple model described above, where such effect is not included.

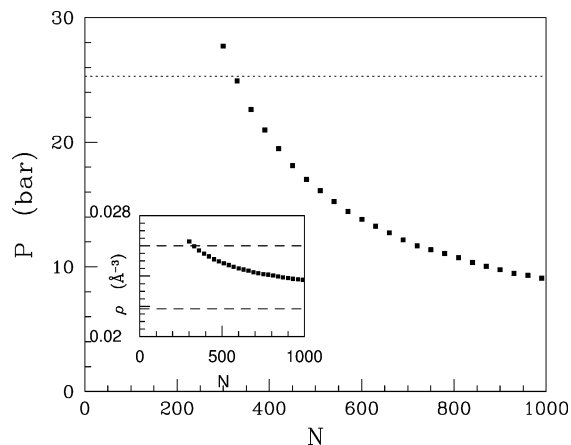


**Figure 1.** Pressure vs size of  ${}^4\text{He}_N$  clusters for the model of scolium discussed in section 2. The dotted line shows the experimental  ${}^4\text{He}$  freezing pressure. The inset shows the corresponding cluster densities as a function of size. The lower and upper dashed lines in the inset show the bulk saturation and freezing densities, respectively.

We will present in the next section more realistic calculations, based on a density functional approach, where the actual  ${}^4\text{He}$  density structure is taken into account and which indicate that indeed the formation of an extended solid core in a scolium made of small  ${}^4\text{He}$  nanodroplets squeezed by the electron is likely to occur.

### 3. Density Functional Calculations

**3.1. Theoretical Method.** We will show in this section that a sufficiently accurate description of the microscopic structure of  ${}^4\text{He}$  around a strongly attractive impurity like a positive ion is indeed possible by using the DF approach widely employed in recent years to study  ${}^4\text{He}$  in confined geometries (for a recent review of applications to helium cluster physics, see ref 34).

We have shown in a previous paper<sup>35</sup> that a modification of the density functional, originally proposed for liquid  ${}^4\text{He}$  by Dalfovo et al.,<sup>31</sup> also accurately describes the solid phase and the freezing transition of liquid  ${}^4\text{He}$  at zero temperature. Without further adjustments, this functional also reasonably describes the interface between the liquid and the (0001) surface of the  ${}^4\text{He}$  crystal,<sup>35</sup> opening the possibility to use unbiased DF methods to address highly inhomogeneous  ${}^4\text{He}$  systems, like droplets doped with strongly attractive impurities or helium adsorbed on strongly attractive substrates. This DF approach represents a valid alternative to a fully quantum description of such highly inhomogeneous and often spatially extended structures, which is computationally very demanding, if not impossible in practice. Our approach is described in detail in refs 32 and 35, and we briefly summarize the main ingredients in the following.

The total energy  $E$  of the electron–helium system can be written as a functional of the electron wavefunction  $\Phi(r)$  and the  ${}^4\text{He}$  “order parameter”  $\Psi(r) = \sqrt{\rho(r)}$ ,  $\rho(r)$  being the  ${}^4\text{He}$  particle density:

$$F[\Psi, \Phi] = \frac{\hbar^2}{2m_4} \int dr |\nabla \Psi(r)|^2 + \int dr f(\rho) + \frac{\hbar^2}{2m_e} \int dr |\nabla \Phi(r)|^2 + \int dr |\Phi|^2 V_{e-\text{He}}(\rho) + \int dr' \rho(r') V_{\text{ion-He}}(r') + \int dr |\Phi(r)|^2 V_{\text{ion-e}}(r) \quad (2)$$

In this equation,  $f(\rho)$  represents the zero temperature potential energy density functional described in ref 35. The  ${}^4\text{He}$  and

electron mass are denoted by  $m_4$  and  $m_e$ , respectively. Inclusion of the electron–helium interaction is done as in ref 32, where the electron–He density-dependent interaction proposed by Cole et al.<sup>33</sup> is used. The ion (which is assumed to be at  $r = 0$ ) is treated as a fixed external potential described by a suitable ion–He pair interaction  $V_{\text{ion-He}}$ , and  $V_{\text{ion-e}}$  represents the ion–electron Coulomb potential. To avoid the singularity in the origin, we assume that the positive charge is uniformly distributed inside a very small, compared with the cluster size, spherical core region (with a radius of  $\sim 1$  Å). We have checked that the solutions do not depend on the radius of this core.

The variational minimization of the above functional yields two coupled Euler–Lagrange equations that have to be solved self-consistently

$$-\frac{\hbar^2}{2m_4} \Delta \Psi + \left\{ \frac{\delta f}{\delta \rho} + |\Phi|^2 \frac{\partial V_{e-\text{He}}(\rho)}{\partial \rho} + V_{\text{ion-He}} \right\} \Psi = \mu \Psi \quad (3)$$

$$-\frac{\hbar^2}{2m_e} \Delta \Phi + \{V_{e-\text{He}}(\rho) + V_{\text{ion-e}}\} \Phi = \epsilon \Phi \quad (4)$$

In the above equations,  $\epsilon$  and  $\mu$  are Lagrange multipliers whose values are determined by the normalization conditions  $\int |\Phi|^2 dr = 1$  and  $\int |\Psi|^2 dr = N$ , with  $N$  being the number of  ${}^4\text{He}$  atoms in the cluster. The iterative solution of the previous equations gives the minimum energy electron and  ${}^4\text{He}$  densities,  $|\Phi|^2$  and  $\rho = |\Psi|^2$ .

**3.2. Ion-Doped  ${}^4\text{He}$  Cluster: DF vs QMC.** We have first checked the accuracy of our theoretical method against “exact” computational schemes such as quantum Monte Carlo methods in the path integral-ground state (PIGS) flavor described in ref 29. For this purpose, we have computed, using both the DF approach described above and the PIGS method as used in ref 24, the structure of a small  ${}^4\text{He}_{70}$  cluster doped with a positive ion. We consider the case of a  $\text{Be}^+$  ion, whose borderline behavior is characterized by the formation of a barely developed solid-like first shell structure (a fully developed, solid-like  ${}^4\text{He}$  snowball forms around the more strongly attractive alkali ions), as opposed to the liquid-like  ${}^4\text{He}$  structure formed around less attractive alkaline-earth ions, like  $\text{Ca}^+$  or  $\text{Mg}^+$ .<sup>24</sup> To model the interaction of the He atoms with the  $\text{Be}^+$  ion,  $V_{\text{ion-He}}$  in eq 2, we have used the ab initio pair potential described in ref 36.

The local  ${}^4\text{He}$  structure around the  $\text{Be}^+$  ion, as computed with our DF approach, is shown in Figure 2 by means of constant  ${}^4\text{He}$  density surfaces, while in Figure 3, we compare the radial  ${}^4\text{He}$  density profile around the  $\text{Be}^+$  ion (solid line) that is the result of the angular average of the density shown in Figure 2, with the results of PIGS calculations (squares). The overall agreement is reasonably good, the main features in the density distribution being correctly reproduced by the DF calculations. Quantitatively, DF tends however to slightly overestimate both the  ${}^4\text{He}$  occupancy in the first shell and the radial position of the second shell.

The helium density in Figure 2 appears to be highly structured, being characterized by 12 high density “blobs” localized in the vicinity of the ion and showing icosahedral symmetry: in Figure 2, one can see from above two pentagonal rings of blobs, rotated by  $\pi/5$  with respect to one another, plus two additional blobs capping the structure (only one is visible in the center of the structure, the other one being hidden by the former). Although one might be tempted to interpret these blobs as representing actual  ${}^4\text{He}$  atoms, it should be kept in mind that



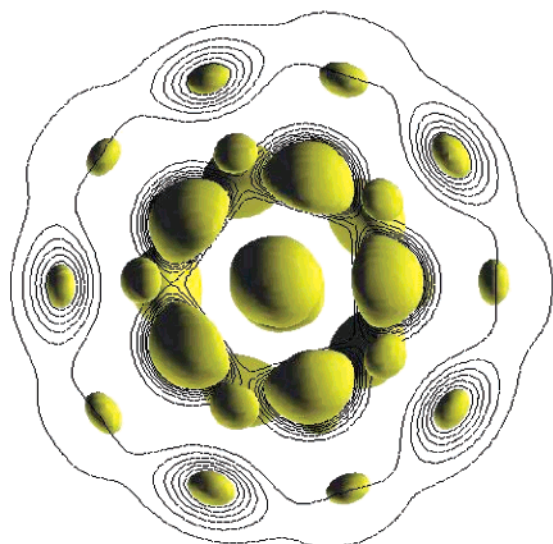


**Figure 2.** Helium density distribution around a  $\text{Be}^+$  ion in a  ${}^4\text{He}_{70}$  cluster, shown by means of surfaces of constant density  $\rho = 0.04 \text{ \AA}^{-3}$ . The lines show equal-density contours in a plane passing through the center of the cluster.

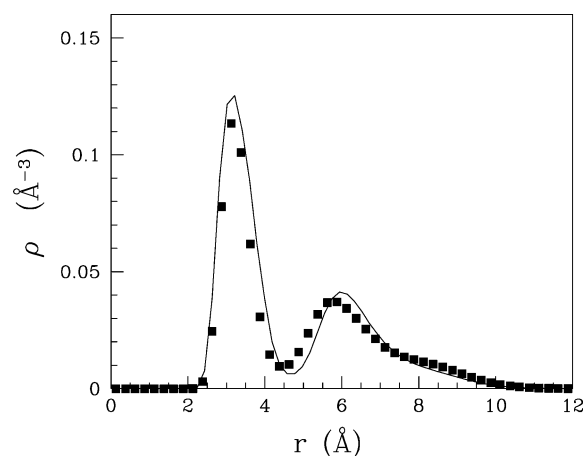


**Figure 3.** Average radial density in a  $\text{Be}^+@{}^4\text{He}_{70}$  cluster. Solid line: DF results. Squares: path integral Monte Carlo results.

what we represent is the squared order parameter  $|\Psi(r)|^2$ . It would be misleading to associate a  ${}^4\text{He}$  atom to each blob in the structure shown in Figure 2. In fact, we have found more than one minimum energy structure of  ${}^4\text{He}$  around the  $\text{Be}^+$ , depending on the initial guess for the density profile used to start the functional minimization. The energies of such configurations are slightly different from one another, by an amount of the order of a few Kelvin. The one shown in Figure 2 is actually the one, among them, with the lowest energy. These structures show a different number of blobs in the first  ${}^4\text{He}$  shell (ranging from 12 to 14), but their radial density profiles are very similar (practically indistinguishable from the one shown in Figure 2); in particular, the integral of the  ${}^4\text{He}$  density distribution within the first solvation shell, which gives the number of  ${}^4\text{He}$  atoms in this shell, is the same in each of these structures.

We note that the density close to the ion in the radial average shown in Figure 3 is characterized by a well-defined inner shell of  ${}^4\text{He}$  atoms around the positive ion. The average density in the first shell is well-above the freezing density of bulk liquid  ${}^4\text{He}$  ( $\rho_f = 0.026 \text{ \AA}^{-3}$ ). Although this might be considered as an indication of a solid-like structure of the  ${}^4\text{He}$  atoms in the first shell, to clearly assess the character, either solid-like or liquid-

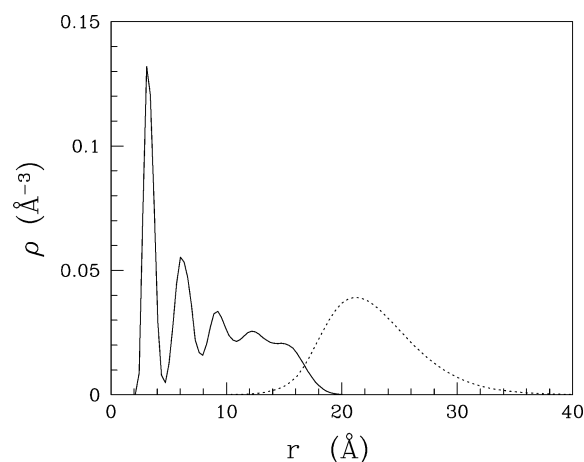


**Figure 4.** Average radial density of a  $\text{Be}^+$  scolium made of 500 helium atoms from DF calculations. Solid line:  ${}^4\text{He}$  density profile in  $\text{Å}^{-3}$ . Dashed line: profile of the electron probability density  $|\Phi|^2$  in arbitrary units.

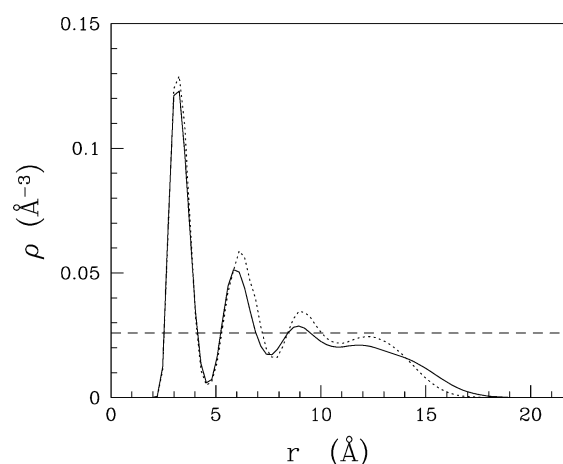


**Figure 5.** Average  ${}^4\text{He}$  radial density. Solid line:  ${}^4\text{He}_{350}$  doped with a  $\text{Be}^+$  ion. Dotted line:  ${}^4\text{He}_{350}$   $\text{Be}^+$  scolium. The dashed line shows the freezing density of bulk liquid  ${}^4\text{He}$ .

like, of the local structure around the ion, one should also consider the dynamical behavior of the helium atoms. One possibility, which has been recently explored, is to analyze the results of path integral Monte Carlo calculations by using suitable imaginary-time-correlation functions.<sup>24</sup>

**3.3. DF Calculations of a Scolium.** In the presence of an extra electron added to the  $\text{Be}^+@{}^4\text{He}_N$  nanodroplet, the minimum energy configuration can be obtained by minimizing the full energy functional described in the previous section. We have investigated two nanodroplet sizes, corresponding to  $N = 350$  and 500.

We show in Figure 4 the radial density profile for both the  ${}^4\text{He}$  distribution (solid line) and the outer electron (dashed line) in the minimum energy configuration. The density of  ${}^4\text{He}$  near the  $\text{Be}^+$  ion is very structured, similar to what occurs for the ion-doped  ${}^4\text{He}$  cluster examined in the previous section.

In order to appreciate the changes induced by the additional electron in the structure of the  ${}^4\text{He}$  nanodroplet, we compare in Figure 5 the radial  ${}^4\text{He}$  density profile with and without the enveloping electron. It appears that (i) the  ${}^4\text{He}$  interface region near the droplet surface is very compressed by the electron with respect to its shape in the ion-doped droplet, and that (ii) the average  ${}^4\text{He}$  density far from the ion increases, reaching the value  $\rho_f = 0.026 \text{ \AA}^{-3}$  which triggers the liquid–solid transition in bulk liquid  ${}^4\text{He}$ .

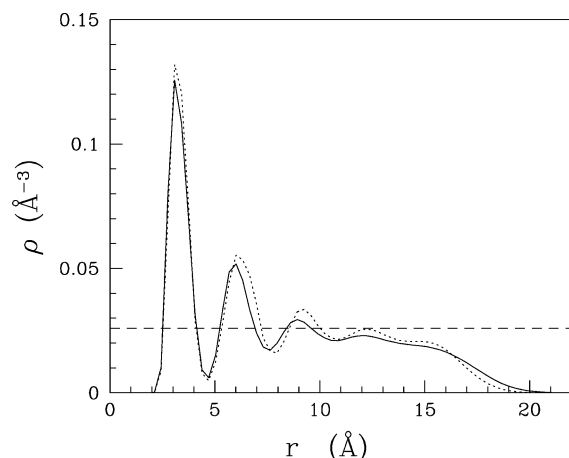


Figure 6. Same as Figure 5 for the  ${}^4\text{He}_{500}$  cluster.

The squeezing effect due to the external electron is actually larger than one might expect judging from the apparently small differences between the two density profiles in Figure 5. Although the number of  ${}^4\text{He}$  atoms in the first shell, defined as the integral of the  ${}^4\text{He}$  density profile in Figure 5 up to the first minimum at  $r \sim 5$  Å, does not increase appreciably in the scolium, the number of  ${}^4\text{He}$  atoms in the second shell increases from 46 (without the electron) to 56 (with the electron). This is a sizable effect, as the electrostatic pressure exerted by the electron forces about 10 more He atoms in the second shell. A compressional effect is also expected in the third and higher order shells, although it is difficult to compute the actual figures being that these shells are not well defined, as it appears from Figure 5.

Additional support to the speculation that the scolium whose density profile is shown in Figure 5 might indeed be solid is based on the observation that its average density is  $3N/(4\pi R^3) \sim 0.027$  Å $^{-3}$ ; that is larger than the freezing density  $\rho_f = 0.026$  Å $^{-3}$  of bulk liquid  ${}^4\text{He}$ . Here, the radius  $R$  of the scolium is defined such that  $\rho(R) = \rho_s/2$ ,  $\rho_s = 0.0218$  being the liquid  ${}^4\text{He}$  density at saturation conditions.

The differences between the  ${}^4\text{He}$  radial density profiles with and without electron are of course more marked in the 350 atom nanodroplet than in the 500 atom one, as it is clear by comparing Figures 5 and 6.

To gain more insight into the structural changes induced in the aspect of the scolium and especially the substantial increase in the number of atoms in the second solvation shell, we have analyzed the angular density distribution within this shell,  $\rho^{2\text{nd}}(\theta, \phi)$ , which is defined as the  ${}^4\text{He}$  density at the point  $(r_2, \theta, \phi)$ ,  $r_2$  being the radial position of the second peak in the density profile of Figure 5.

This quantity is shown in Figure 7 for the  $\text{Be}^+@{}^4\text{He}_{350}$  nanodroplet and in Figure 8 for the corresponding scolium. The appearance of ordered peaks in the  $\rho^{2\text{nd}}(\theta, \phi)$  plots in Figure 7 reveals a structural order within this shell. In the case of a scolium (Figure 8), the number of peaks increases, corresponding to the already noticed increase in the second-shell occupancy, while the structure appears to be less ordered than in the  $\text{Be}^+@{}^4\text{He}_{350}$  nanodroplet.

Our analysis indicates that the  ${}^4\text{He}$  droplet inner region may turn solid under the electron pressure, while small droplets may be completely solid. As already pointed out, however, from the static density profile alone, it is not possible to assess the degree of localization of the  ${}^4\text{He}$  atoms and, in particular, to discriminate between solid-like versus liquid-like behavior within the individual solvation shells. A clear conclusion about the

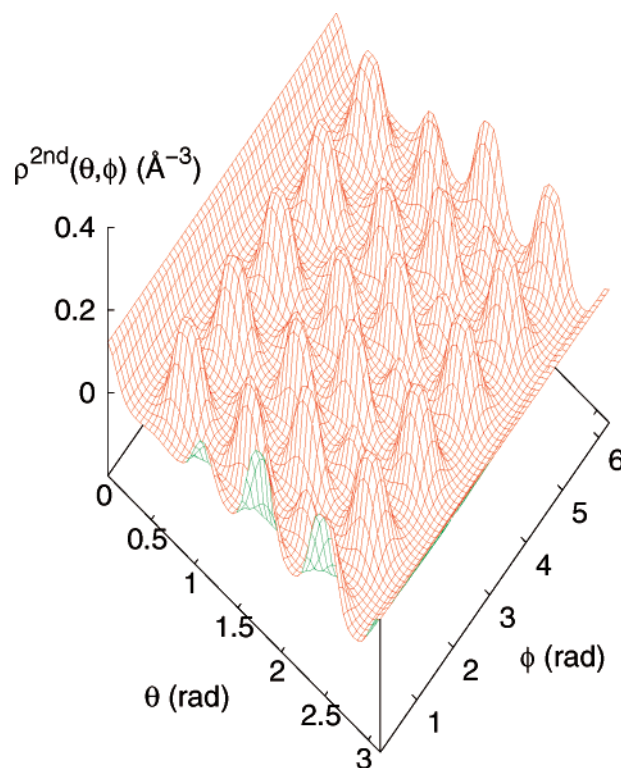


Figure 7. Angle-resolved density profile in the second shell of a  $\text{Be}^+@{}^4\text{He}_{350}$  droplet.

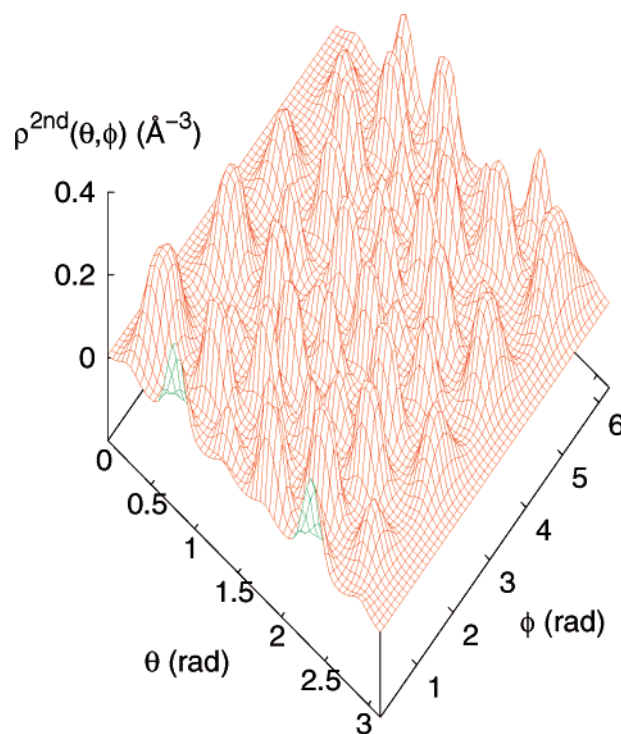


Figure 8. Same as Figure 7 for the  $\text{Be}^+@{}^4\text{He}_{350}$  scolium.

“solidity” of a scolium could only be revealed by using some dynamical criterion (like, e.g., the one described in ref 24), involving temporal correlations between the atom positions in the droplet, something which is not possible within the static DF approach used here.

#### 4. Stability of a Scolium

There are basically two process which can limit the lifetime of a scolium: (i) the tunneling of the electron into the helium,

with subsequent neutralization of the positive charge of the ion, and (ii) the drift of the positive ion to the surface caused by the electric field of the electron. The combination of these two effects could make the rate of electron–ion recombination so fast as to prevent the experimental observation of a scolium (we do not consider here other mechanisms, related to the helium and electron density fluctuations, including loss of  $^4\text{He}$  atoms, which might also affect the recombination process).

The former process is characterized by a lifetime that, approximating the actual e–He potential with a rectangular barrier, increases exponentially as  $\tau_0 \exp[2d\alpha]$ , where  $\alpha = \sqrt{2m_e V_0/\hbar^2}$  and  $d$  is the effective width of the e–He potential barrier. The prefactor  $\tau_0$  is related to the inverse of an attempt frequency  $\nu \sim E_{\min}/\hbar$ , with  $E_{\min}$  being a characteristic electron energy. For sufficiently large clusters, tunneling of the electron into the ion core region is largely inhibited because the tunnel penetration depth is of the order of a few angstrom, that is, much smaller than the thickness of the e–He potential barrier. This can be seen in the actual results of our calculations: in Figure 4, it appears that the electron wavefunction decays quite rapidly inside the  $N = 500$  cluster interior. We have numerically estimated  $\alpha$  from the exponential tail of the electron density amplitude shown in Figure 4. We find  $\alpha = 0.36 \text{ \AA}^{-1}$ . We compute the prefactor  $\tau_0$  using  $E_{\min} \sim E_{\text{kin}}/2$ , with  $E_{\text{kin}}$  being the electron kinetic energy. This gives  $\tau_0 \sim 1.6 \times 10^{-13} \text{ s}$ . The effective barrier width,  $d \sim 14.3 \text{ \AA}$ , can be read directly from the  $^4\text{He}$  density profile in Figure 4. We obtain a tunnel lifetime  $\tau \sim 5 \times 10^{-9} \text{ s}$ , that is, a sufficiently long time to allow for an experimental detection of a scolium. A similar estimate, done for the case of the smaller  $N = 350$  cluster, gives  $\tau \sim 0.3 \times 10^{-9} \text{ s}$ .

The second recombination mechanism has to do with the ion mobility in a very dense  $^4\text{He}$  system, which could be very small. The stability of the ion core with respect to changes from its equilibrium position in the cluster center has been addressed by Golov and Sekatskii<sup>4</sup> using perturbation theory within a simple model of a scolium, and it has been found that the ion core is in a stable state, with small mean-square displacements about this position. These authors considered two contributions to the energy change as the cationic core of the scolium Rydberg is moved from the center of the helium droplet. One is electrostatic, basically, the ion-induced dipole interaction of the bare cation with the helium which produces a weak confinement potential with a minimum at the center of the droplet. This potential was discussed in more depth by Lehmann and Northby.<sup>37</sup> The force constant of this potential for small displacements from the center is  $+0.75/N \text{ (N/m)}$ .

A second contribution to the energy of a scolium comes from the change in the energy of the Rydberg electron. Golov and Sekatskii estimated this by assuming that the wavefunction for the Rydberg electron stayed centered on the moving cation but was otherwise unchanged. This model predicts a strong repulsive interaction as the electron density is dragged into the helium. However, since it ignores the change in the spatial distribution of the highly polarizable Rydberg electron, it does not realistically address the stability issue. In the following, we approach the problem perturbatively, within the simple model already described in section 2. For a small cation displacement (relative to the size of the droplet)  $a$ , the problem is equivalent to the original Coulomb potential but with the addition of a dipole at the core of magnitude  $\mu = ea$ .

Golov and Sekatskii showed that asymptotically, the Rydberg series of a scolium have  $l$  independent quantum defects  $\delta = (1/\pi) \sqrt{8R/a_0} - (1/4)$ , where  $a_0$  is the Bohr radius. This

implies that the hydrogenic degeneracy holds and that the analysis of the effect of core multipole moments given by Watson<sup>38</sup> holds. Watson showed that the second-order energy correction (in atomic units) for a core dipole can be written

$$E(n,l,m) = \frac{\mu^2[l(l+1) - 3m^2]}{(2l+3)(2l-1)l(l+1)} \langle 1/r^2 \rangle_{nlm} \quad (l > 0) \quad (5)$$

$$E(n,0,0) = -\frac{\mu^2}{3} \langle 1/r^2 \rangle_{n00} \quad (l = 0) \quad (6)$$

The  $[l(l+1) - 3m^2]$  factor, like that found in the second-order Stark effect of a linear rotor, means that, for all  $l > 0$ , the energy levels will be split, preserving the mean energy, but with  $m = 0$  at the highest energy and  $m = l$  at the lowest. The  $l = 0$  states will have an energy that decreases upon displacement of the ion from the center and this will overwhelm the interaction of the ion with the helium except for very high Rydberg states ( $\langle r^{-2} \rangle \sim n^{-3}$ ). For a droplet of  $N \sim 10^4$ , the size of the electronic contribution to the energy is  $\sim 10^3$  times larger than the ion–helium induced dipole interaction that holds the ion to the droplet center.

For the lowest lying Rydberg states with the electron outside the droplet, the  $l$  degeneracy is lifted and the Watson expressions do not directly apply. We have numerically found the energy levels by matching the boundary conditions for the analytic hydrogenic wavefunctions inside and outside the droplet. The effect of core dipole was then calculated from these solutions. It was found that the lowest scolium state is unstable with a sizable negative force constant. As the cation moves off center, the electron density localizes on the side of the displacement, pulling the cation toward the surface and thus likely leading to rapid charge neutralization. One can estimate the time for such neutralization as a few times the inverse of the magnitude of the imaginary frequency, and this is predicted to be on the order of a few picoseconds for a droplet with  $R \sim 100a_0$  ( $N \sim 14\,000$ ). This suggests that for the large droplets a scolium will be quite short-lived and likely difficult to directly detect. However, for smaller droplets, which this work has demonstrated will have a fairly large solid core, the forces holding the cation in the center of the droplet will be much larger.

## 5. Summary

We have investigated, by means of density functional calculations, the structure of a scolium, that is, an electron circulating around a positively charged  $^4\text{He}$  nanodroplet, temporarily prevented from neutralization by the helium–electron repulsion. The outer electron enveloping the nanodroplet in a scolium exerts an additional electrostatic pressure which further increases the local  $^4\text{He}$  density around the core. We suggest, on the basis of our results, that under such pressure small  $^4\text{He}$  clusters may turn solid.

Our DFT approach, being a static one, cannot help in precisely determining the character (solid-like or liquid-like) of the helium surrounding the impurity ion. Other, dynamical schemes should be used to this purpose, such as the path integral Monte Carlo method used in ref 24, although the relevant size of a scolium system may make a fully microscopic calculation unpractical. We nevertheless believe that our results, in particular, the observed increase in the “packing” of helium atoms in the region occupied by the ion, give a strong indication that an extended core region of a scolium, larger than the usual snowball found around positive ions in liquid  $^4\text{He}$ , is probably solid and that sufficiently small scoliums may be solid altogether.



A key issue is how a solid scolium might be experimentally detected. The problem is to unambiguously ascertain whether this system is solid or not and this is probably as challenging a problem for the experimentalists as for the theoreticians. We propose here two different kind of experiments that might solve this problem, whose interpretations however will critically depend on accurate model calculations.

Local high-density structures of  $^4\text{He}$  around neutral impurities are known to have a detectable effect on experimental measures. For instance, recent experimental measurements<sup>40</sup> of fluorescence spectra of Cs impurities implanted in solid  $^4\text{He}$  show features that are not present when the atom is implanted in bulk liquid  $^4\text{He}$ , and which are attributed to the formation of exciplexes in which several  $^4\text{He}$  atoms are tightly arranged on a ring around the waist of the excited electronic distribution of the impurity. We suggest that a similar experiment, based on the electronic excitation of the ion in a scolium, could hopefully reveal the existence of a solid scolium.

The rotation of linear molecules embedded in  $^4\text{He}$  clusters is known not to be hindered by the superfluid phase, resulting in a well-resolved rotational structure,<sup>39</sup> however, with an increased effective moment of inertia due to some  $^4\text{He}$  atoms dragged by the rotating molecule. A similar but more complex experiment measuring the rotational spectrum of a (positively charged) linear molecule trapped in a scolium (whose outer electron has been provided by Rydberg excitation of the embedded molecule) could reveal the character of the embedding helium, a solid structure being signalled by a much larger value of the measured moment of inertia of the molecule.

**Acknowledgment.** We thank G. Scoles, C. Callegari, K. von Haeften, M. Drabbels, A. Golov, S. Sekatskii, and F. Toigo for useful comments and discussions. We thank S. Paolini for providing the PIMC results reported in this paper. This work has been performed under Grant FIS2005-01414 from DGI, Spain (FEDER), Grant 2005SGR00343 from Generalitat de Catalunya, and under the HPC-EUROPA project (RII3-CT-2003-506079), with the support of the European Community-Research Infrastructure Action under the FP6 "Structuring the European Research Area" Programme.

## References and Notes

- (1) Chalupa, J. *Solid State Commun.* **1982**, *44*, 219.
- (2) Lerner, P. B.; Sokolov, I. M. *Z. Phys. D* **1989**, *14*, 173.
- (3) Sekatskii, S. K. *Physica Scripta* **1998**, *57*, 313.
- (4) Golov, A.; Sekatskii, S. Z. *Phys. D* **1993**, *27*, 349.
- (5) Scoles, G., unpublished.
- (6) Stienkemeier, F.; Lehmann, K. K. *J. Phys. B* **2006**, *39*, R127.
- (7) von Haeften, K.; Laarmann, T.; Wabnitz, H.; Moller, T. *J. Phys. B* **2005**, *38*, S373.
- (8) Peterka, D. S.; Lindinger, A.; Poisson, L.; Ahmed, M.; Neumark, D. M. *Phys. Rev. Lett.* **2003**, *91*, 043401.
- (9) von Haeften, K.; de Castro, A. R. B.; Joppien, M.; Moussavizadeh, L.; von Pietrowski, R.; Moller, T. *Phys. Rev. Lett.* **1997**, *78*, 4371; von Haeften, K.; Laarmann, T.; Wabnitz, H.; Moller, T. *Phys. Rev. Lett.* **2001**, *87*, 153403.
- (10) von Haeften, K.; Fink, K. *Eur. Phys. J. D* **2007**, *43*, 121.
- (11) Claas, P.; Mende, S. O.; Stienkemeier, F. *Rev. Sci. Instrum.* **2003**, *74*, 4071.
- (12) Gspann, J. *Physica B* **1991**, *169*, 519.
- (13) Northby, J. A.; Kim, C.; Jian, T. *Physica B* **1994**, *197*, 426.
- (14) Farnik, M.; Samelin, B.; Toennies, J. P. *J. Chem. Phys.* **1999**, *110*, 9195.
- (15) Hernando, A.; Mayol, R.; Pi, M.; Barranco, M.; Ancilotto, F.; Bünermann, O.; Stienkemeier, F. *J. Phys. Chem. A* **2007**, *111*, 7303.
- (16) Federmann, F.; Hoffmann, K.; Quaas, N.; Close, J. D. *Phys. Rev. Lett.* **1999**, *83*, 2548.
- (17) Wittig, C., private communication.
- (18) Loginov, E.; Drabbels, M. *J. Phys. Chem. A* **2007**, *111*, 7504.
- (19) Drabbels, M., private communication.
- (20) Cole, M. W.; Toigo, F. *Phys. Rev. B* **1978**, *17*, 2054.
- (21) Atkins, K. R. *Phys. Rev.* **1959**, *116*, 1339.
- (22) Cole, M. W.; Bachman, R. A. *Phys. Rev. B* **1977**, *15*, 1388.
- (23) Rossi, M.; Verona, M.; Galli, D. E.; Reatto, L. *Phys. Rev. B* **2004**, *69*, 212510.
- (24) Paolini, S.; Ancilotto, F.; Toigo, F. *J. Chem. Phys.* **2007**, *126*, 124317.
- (25) Toennies, J. P.; Vilesov, A. F. *Angew. Chem., Int. Ed.* **2004**, *43*, 2622.
- (26) Buchenau, H.; Toennies, J. P.; Northby, J. A. *J. Chem. Phys.* **1991**, *95*, 8134.
- (27) Buzzacchi, M.; Galli, D. E.; Reatto, L. *Phys. Rev. B* **2001**, *64*, 094512.
- (28) Lehmann, K. K. *Phys. Rev. Lett.* **2002**, *88*, 145301.
- (29) Sarsa, A.; Schmidt, K. E.; Magro, W. R. *J. Chem. Phys.* **2000**, *113*, 1366.
- (30) This is the energy cost required to create a quasi-free electron state inside bulk  $^4\text{He}$ . There is however another possible state where the electron becomes localized inside a cavity, whose energy cost is lower ( $\sim 0.22$  eV).<sup>32</sup> As a consequence, one should in principle consider the possibility of more complex paths in the multi-dimensional energy surface along which the energy barrier felt by the electron could be lower than 1 eV. We have not considered here such possibility.
- (31) Dalfovo, F.; Lastris, A.; Pricapenko, L.; Stringari, S.; Treiner, J. *Phys. Rev. B* **1995**, *52*, 1193.
- (32) Grau, V.; Barranco, M.; Mayol, R.; Pi, M. *Phys. Rev. B* **2006**, *73*, 064502.
- (33) Cheng, E.; Cole, M. W.; Cohen, M. H. *Phys. Rev. B* **1994**, *50*, 1136; Cheng, E.; Cole, M. W.; Cohen, M. H. *Phys. Rev. B* **1994**, *50*, 16134, erratum.
- (34) Barranco, M.; Guardiola, R.; Hernández, S.; Mayol, R.; Pi, M. *J. Low Temp. Phys.* **2006**, *142*, 1.
- (35) Ancilotto, F.; Barranco, M.; Caupin, F.; Mayol, R.; Pi, M. *Phys. Rev. B* **2005**, *72*, 214522.
- (36) Bellert, D.; Beckenridge, W. H. *Chem. Rev.* **2002**, *102*, 1595.
- (37) Lehmann, K. K.; Northby, J. A. *Mol. Phys.* **1999**, *97*, 639.
- (38) Watson, J. K. G. *Mol. Phys.* **1994**, *81*, 277.
- (39) Grebenev, S.; Toennies, J. P.; Vilesov, A. F. *Science* **1998**, *279*, 2083.
- (40) Nettel, D.; Hofer, A.; Moroshkin, P.; Müller-Siebert, R.; Ulzega, S.; Weis, A. *Phys. Rev. Lett.* **2005**, *94*, 63001.